Research Article | Vol. 27, No. 8 | 15 Apr 2019 | OPTICS EXPRESS A458
Optics EXPRESS

Enhanced performance of InGaN/GaN MQW LED with strain-relaxing Ga-doped ZnO transparent conducting layer

SANG-JO KIM,[1] KWANG JAE LEE,[1] SEMI OH,[1] JANG-HWANG HAN,[1] DONG-SEON LEE,[2,3] AND SEONG-JU PARK[1,4]

[1]*School of Materials Science and Engineering, Gwangju Institute of Science and Technology, Gwangju 61005, South Korea*
[2]*School of Electrical Engineering and Computer Science, Gwangju Institute of Science and Technology, Gwangju 61005, South Korea*
[3]*dslee66@gist.ac.kr*
[4]*sjpark@gist.ac.kr*

Abstract: We report the enhanced optical and electrical properties of InGaN/GaN multiple quantum well (MQW) light-emitting diodes (LEDs) with strain-relaxing Ga-doped ZnO transparent conducting layers (TCLs). Ga-doped ZnO was epitaxially grown on *p*-GaN by metal–organic chemical vapor deposition. The optical output power of a LED with a 500-nm-thick-Ga-doped ZnO TCL increased by 30.9% at 100 mA, compared with that of an LED with an indium tin oxide (ITO) TCL. Raman spectroscopy measurement and the simulation of wavefunction overlap of electron and hole in MQWs revealed that the enhanced optical output power was attributed to the increased internal quantum efficiency due to the decreased compressive strain in the active region. The increase of optical output was also attributed to the increased optical transmittance of the Ga-doped ZnO TCL owing to its higher refractive index compared to that of ITO TCL. Furthermore, the forward voltage of LED with a Ga-doped ZnO TCL was lower than that of LED with an ITO TCL because of the increased carrier concentration and mobility in the Ga-doped ZnO TCL.

1. Introduction

The development of high-efficiency InGaN/GaN multiple quantum well (MQW) light-emitting diodes (LEDs) has progressed markedly and they have been used extensively in many applications such as backlight units, full color displays, automotive lighting, and general illumination [1,2]. Although InGaN/GaN MQW LEDs are commercially available, their internal quantum efficiency (IQE) and light extraction efficiency (LEE) require further improvement to realize high-efficiency and high-power LEDs. IQE is strongly influenced by threading dislocations originated from the mismatch of the lattice constants and thermal expansion coefficients of GaN and the underlying sapphire substrate. These threading dislocations act as nonradiative recombination centers, suppressing emission from nearby quantum wells (QWs). IQE is also lowered by the separation of the electron and hole wave functions driven by the polarization-induced internal electrostatic field [3]. According to Snell's law, LEE is limited by the total internal reflection caused by the large difference in the refractive index (n) of GaN (n = 2.4) and air (n = 1). In addition, the light within the escape cone of GaN-based LEDs undergoes Fresnel reflection [4]. Extensive investigations have been performed to improve both the IQE and LEE of LEDs using epitaxial lateral overgrowth, surface plasmons, bandgap engineering, photonic crystals, and surface texturing [5–9].

Indium tin oxide (ITO) has emerged as one of the most promising materials for use as the transparent conducting layer (TCL) in GaN-based LEDs because of its low resistivity and high transparency in the visible wavelength region. However, indium is an expensive rare

#359953 https://doi.org/10.1364/OE.27.00A458
Journal © 2019 Received 11 Feb 2019; revised 13 Mar 2019; accepted 13 Mar 2019; published 20 Mar 2019

Optics EXPRESS

metal and the limited thermal stability of ITO raises concerns about its use in high power LED chips. ZnO has been investigated as an alternative to ITO for use as the TCL material in GaN-based LEDs. Compared with ITO, ZnO boasts the advantages of higher transmittance, lower resistivity, improved temperature stability, lower cost, and non-toxicity [10]. And the high refractive index of ZnO-based TCLs enhances LEE [11,12]. One of the important merits of ZnO is its epitaxial growth on *p*-GaN [13]. In particular, Ga-doped ZnO was found to be more appropriate to develop TCLs for GaN-based LEDs compared to Al- and In-doped ZnO because of the lower oxidation reactivity of Ga than those of Al and In and the smaller difference between the bond lengths of Ga-O and Zn-O than those between Zn-O and Al-O or In-O [14]. In addition, ZnO nanorods (NRs) were used as additional structures to improve the light extraction in GaN-based LED. Leem et al. reported that the light extraction of LED was improved by reducing the difference in refractive index between *n*-GaN and air in vertical LEDs by using ZnO NRs [15]. And it was also reported that the light extraction of LEDs was improved by using SiO_2-coated ZnO NR arrays on ITO TCL due to the reduced Fresnel reflection [16]. Although ZnO-based TCLs have been shown that the light extraction is improved, the influence of ZnO TCLs on IQE has not yet been studied. Recently, Park et al. reported that an Sb-doped *p*-ZnO layer epitaxially grown on an InGaN/GaN MQW layer using metal–organic chemical vapor deposition (MOCVD) relaxed the compressive strain in the LED active region [17]. Strain relaxation occurred because the lattice constant of ZnO is slightly (1.8%) larger than that of GaN, which generates tensile strain and compensates for the compressive strain in the InGaN active region resulting from the lattice mismatch of InGaN and GaN in the MQWs. However, the optical output power of an LED with the hybrid structure *p*-ZnO/(InGaN/GaN) MQW/*n*-GaN was much lower than that of a conventional GaN-based LED because of the poor current spreading in the columnar-structured Sb-doped *p*-ZnO layer.

In this study, we investigate the performance of InGaN/GaN MQW LEDs with strain-relaxing Ga-doped ZnO TCLs. We find that the optical output power of LEDs with 180- and 500-nm-thick Ga-doped ZnO TCLs is greatly enhanced by 26.9% and 30.9% at 100 mA, respectively, compared to that of LEDs with ITO TCLs. The Ga-doped ZnO TCL epitaxailly grown on *p*-GaN introduces tensile strain into MQWs and this compensates the compressive strain in the MQW active region resulting from lattice mismatch of InGaN and GaN. This led to the relaxation of strain and increased wavefunction overlap between electron and hole. The large increase of optical output power is attributed to the increased IQE resulting from the relaxation of compressive strain in the active region and increased light extraction.

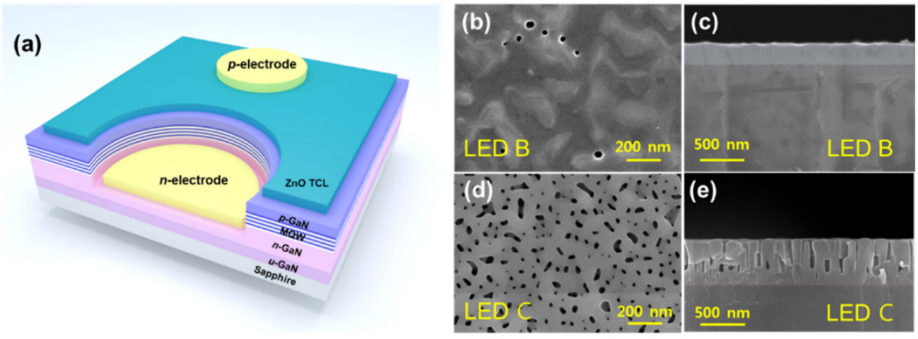

Fig. 1. (a) Schematic of an LED with a Ga-doped ZnO TCL. Top-view and cross-sectional SEM images of Ga-doped ZnO TCLs with thicknesses of (b), (c) 180 nm (LED B) and (d), (e) 500 nm (LED C).

Optics EXPRESS

2. Experiment

The LEDs were grown on a c-plane (0001) sapphire substrate by MOCVD. The LED structure consisted of a GaN buffer layer grown at low temperature, highly Si-doped *n*-type GaN layer, InGaN/GaN MQW active layer with an emission wavelength of 460 nm, and Mg-doped *p*-type GaN layer. The LED wafer was patterned by photolithography and then the LEDs were etched until the *n*-GaN layer was exposed using inductively coupled plasma with CH_4 and Cl_2 as source gases. On top of *p*-GaN layer, a 180- or 500-nm-thick Ga-doped ZnO film (denoted as LED B and LED C. respectively) was deposited at a pressure of 50 Torr and growth temperature of 650 °C using a separate ZnO MOCVD system. Diethylzinc (DEZn), oxygen (O_2), and triethylgallium (TEGa) were used as the Zn, O_2, and *n*-type Ga doping source, respectively. The flow rates of DEZn, O_2, and TEGa were 20.1, 0.33, and 17 nmol/min, respectively. During the growth of the ZnO layer on *p*-GaN by MOCVD, the $ZnGa_2O_4$ phase formed at the ZnO/*p*-GaN interface, which degrades electrical performance because of its high resistivity at room temperature [18]. The Ga-doped ZnO TCL was annealed at 700 °C in a nitrogen/air atmosphere for 1 min to remove $ZnGa_2O_4$. To fabricate an LED chip with a size of 350 × 350 μm, the Ga-doped ZnO TCL was partially etched in a dilute HCl solution to form electrode pads and then Ti/Au (30/80 nm) layers were deposited as *n*- and *p*- contacts, respectively, as shown in Fig. 1(a). Figure 1(d)-1(e) display top-view and cross-sectional scanning electron microscopy (SEM) images of 180- and 500-nm-thick Ga-doped ZnO TCLs grown on *p*-GaN. The 180-nm-thick Ga-doped ZnO layer grew epitaxially on *p*-GaN and contained small hexagonal-shaped pits [Fig. 1(b) and 1(c)]. The 500-nm-thick Ga-doped ZnO film contained many nanosized pits [Fig. 1(d) and 1(e)]. To compare optical and electrical properties, a 180-nm-thick ITO TCL was deposited on a *p*-GaN layer and used to fabricate a reference LED (denoted as LED A). Raman scattering measurements were conducted to study the difference in strain in the InGaN/GaN MQW structure with and without a Ga-doped ZnO TCL deposited on *p*-GaN, as shown in Fig. 2(a). Excitation at 514 nm and a power of 2.4 mW using an Ar + laser line was employed for the Raman measurements.

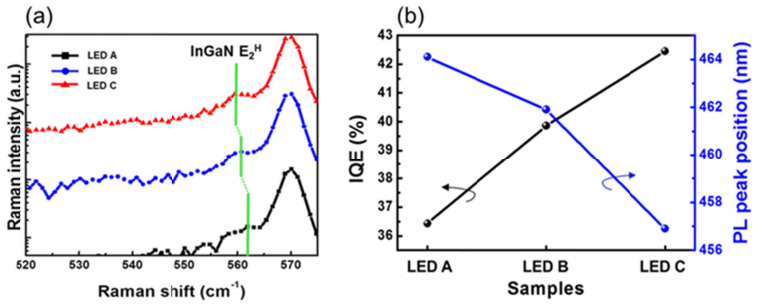

Fig. 2. (a) Room-temperature Raman spectra and (b) IQE and PL peak positions for LED A, B, and C.

3. Results and discussion

Figure 2(a) shows that there are two resolved phonon modes in each Raman spectrum of LED A, B, and C. The peak near 570 cm^{-1} is from the E_2^H mode of the strained hexagonal GaN and the shoulder (indicated by a green line) located near the 560 cm^{-1} peak originates from the strained InGaN E_2^H mode. The InGaN E_2^H phonon peaks for LED B and LED C were observed at 560.7 and 559.6 cm^{-1}, respectively, whereas that of LED A appeared at 561.8 cm^{-1}, as shown in Fig. 2(a). The Raman spectra show that the InGaN E_2^H phonon peak of LED C is slightly redshifted from that of LED B. This result indicates that the compressive

Optics EXPRESS

strain in the active region should be further relaxed with increasing thickness of the Ga-doped ZnO.

To further understand the strain relaxation induced by the Ga-doped ZnO TCL, we calculated the biaxial strain ($\varepsilon_{\parallel}$) based on the Raman spectral shift. The wave number shift of the phonon mode in Raman spectra can be correlated with $\varepsilon_{\parallel}$ according to the following Eq. (1) [18],

$$\Delta\omega = \omega - \omega_0 = (2\alpha_\lambda - 2\frac{c_{13}}{c_{33}})\varepsilon_{\parallel} \quad (1)$$

where ω is the wave number of the InGaN E_2^H signal of the LED, ω_0 is the wave number of the E_2^H signal of the strain-free InGaN layer (555 cm^{-1}) [19], α_λ and b_λ are phonon deformation potentials, and c_{13} and c_{33} are elastic constants. The values of α_λ , b_λ , c_{13} , and c_{33} were obtained from a linear interpolation of InN and GaN [20,21]. According to Eq. (1), $\varepsilon_{\parallel}$ of LED A, B, and C were calculated to be −6.76%, −5.67%, and −4.57%, respectively. This result indicates that the compressive strain induced by the lattice mismatch between the InGaN and GaN layers in the MQWs was relaxed by the Ga-doped ZnO TCL grown epitaxially on *p*-GaN.

The relaxation of compressive strain in the active region by the Ga-doped ZnO TCL led to not only a blueshift of the photoluminescence (PL) peak wavelength but also increased IQE, as shown in Fig. 2(b). The peak wavelength of PL was measured by an He-Cd (325 nm) laser and IQE was estimated from the temperature dependence of PL intensity by assuming that IQE was 100% at a low temperature of 10 K [22]. Figure 2(b) reveals that the PL peak positions of LED A, B, and C appeared at 464.1, 461.9, and 456.9 nm, respectively, and that the IQEs of LED B and C were improved by 9.4% and 16.5%, respectively, compared to that of LED A. The blueshift of PL peak and enhanced IQE are attributed to the increased radiative recombination rates caused by the increased overlap of electron and hole wave functions owing to the reduced quantum-confined Stark effect (QCSE) in the active region of LED B and C compared with that of LED A [23]. These results are well agreed with previous studies on the IQE enhancement by strain relaxation in LEDs [24–26].

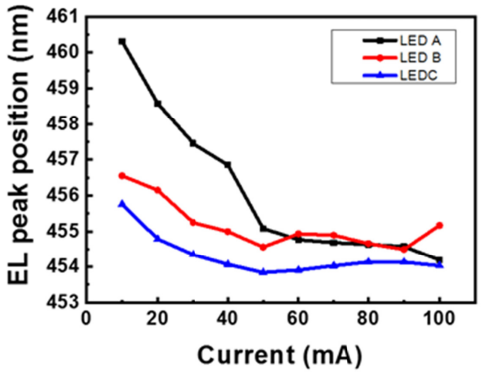

Fig. 3. EL peak position as a function of current for LED A, B, and C.

Figure 3 shows that the electroluminescence (EL) peak positions for LED A, B, and C at 10 mA appeared at 460.3, 456.5, and 455.7 nm, respectively. In addition, the EL peaks of LED A, B, and C shifted with increasing injection current from 10 to 100 mA at room temperature. LED A featured the largest blueshift of 6.13 nm with increasing forward current from 10 to 100 mA. This behavior resulted from the screening effect of the piezoelectric field

Optics EXPRESS

in the MQWs by the injected carriers and the carriers moving up to a higher energy level with increasing injection current [27]. LED B and C displayed smaller blueshift of 1.99 and 1.93 nm, respectively. These smaller blueshift is attributed to the decrease of the piezoelectric field in InGaN/GaN MQWs induced by the Ga-doped ZnO TCL compared to the case for the LED with an ITO TCL.

To further investigate how the Ga-doped ZnO TCL affected the piezoelectric polarization of the LEDs, the wave function overlap of electrons and holes and energy-band diagrams of the LED A and C at 100 mA were calculated based on the carrier transport model using SiLENse 5.4 (STR software). Material parameters used in the simulation can be found in the literature [28]. Figure 4(a) and 4(b) show the energy bands of LED A and C at 100 mA, respectively. The energy bands are slightly bent in the *p*-GaN layer because of the tensile strain introduced by the Ga-doped ZnO TCL [Fig. 4(b)]. The valence bands of *p*-GaN in LED A and C are compared in Fig. 4(c). The energy of the valence band of *p*-GaN in LED C is increased by over 179 meV compared with that of LED A. It has been reported that the valence band energy of *p*-GaN is increased because of the decreased energy band bending resulting from the strain relaxation [29]. In addition, the valence band energy on right side of *p*-GaN in LED C is further increased by 171 meV compared with that on the left side of *p*-GaN. These results indicate that the holes injected from the Ga-doped ZnO layer are efficiently accumulated in *p*-GaN and transported into MQWs, resulting in a large increase in optical output power.

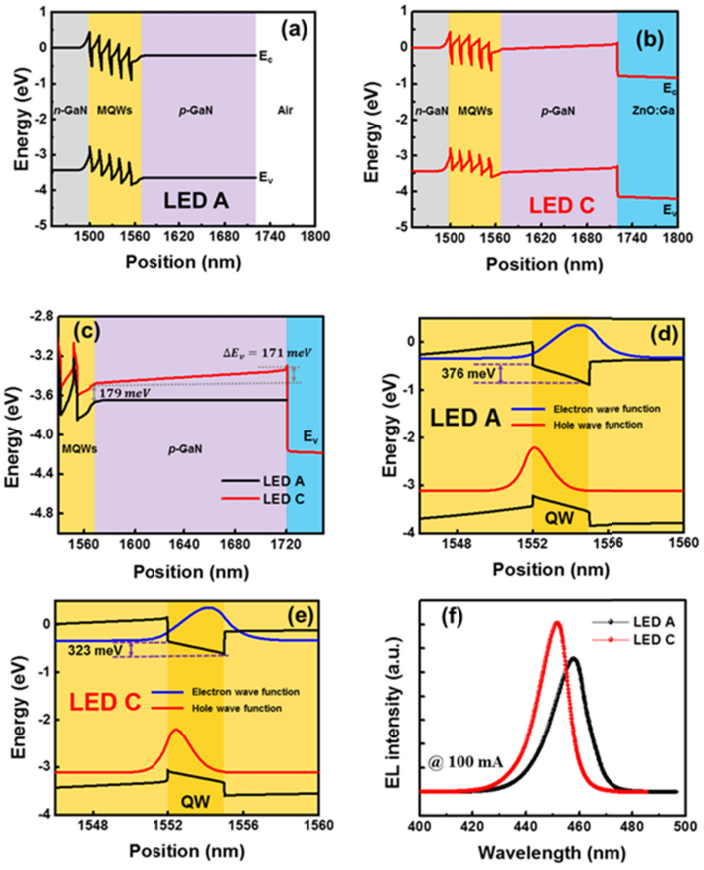

Fig. 4. Energy-band diagrams of (a) LED A and (b) LED C at 100 mA. (c) Enlarged energy-band diagrams of LED A and C around the *p*-GaN layer. Calculated electron and heavy hole

wave-function overlap of QWs adjacent to the *p*-GaN region for (d) LED A and (e) LED C. (f) Calculated EL intensities for LED A and C.

The tensile strain generated by the Ga-doped ZnO TCL can also affect the MQW region. The energy bands and carrier wave function overlaps in QWs adjacent to *p*-GaN in LED A and C are presented in Fig. 4(d) and 4(e), respectively. The band bending in the conduction band of the QW in LED A is 376 meV, which decreases to 323 meV in LED C because of the compressive strain. The wave function overlap of electrons and holes increases from 32.7% for LED A to 37.6% for LED C. The increased wavefunction overlap increases the IQE as shown in Fig. 2(b) and enhances the EL intensity; the EL intensity of LED C at 100 mA is 13.4% higher than that of LED A, as illustrated in Fig. 4(f). The EL peak position for LED C is also blueshifted by 6.3 nm compared with that of LED A. These results are attributed to the decreased QCSE resulting from the lower compressive strain in the MQWs in the LEDs with a Ga-doped ZnO TCL compared with the case for the ITO-based LED.

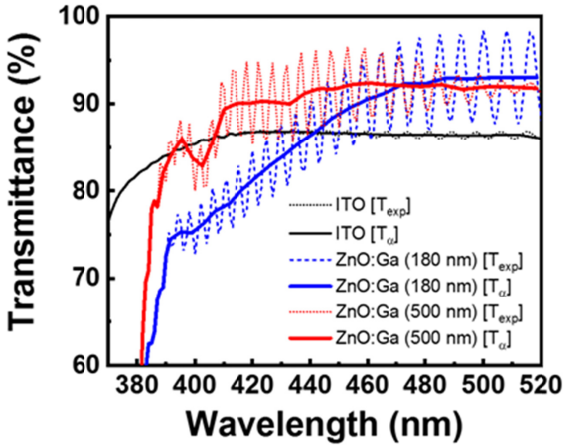

Fig. 5. Transmittance spectra of 180-nm-thick ITO and 180-and 500-nm-thick Ga-doped ZnO films on GaN/double-polished sapphire substrates.

To investigate the optical propert0ies of ITO and Ga-doped ZnO TCLs, we measured the transmittance of 180-nm-thick ITO and 180- and 500-nm-thick Ga-doped ZnO layers deposited on GaN/double-polished sapphire substrates, as shown in Fig. 5. Oscillations in optical transmittance spectra are related to the internal structure of the material, namely, the presence of a semiconductor-insulator interface. The interference-free transmission (T_α) was calculated from the following Eq. (2) [30,31],

$$T_\alpha = (T_{\max} \cdot T_{\min})^{1/2} \tag{2}$$

where T_{max} and T_{min} are the maximum and minimum transmittance at one interference cycle, respectively. The transmittance of ITO and 180- and 500-nm-thick Ga-doped ZnO at 460 nm is 86.8%, 92.5%, and 88.8%, respectively. The reported refractive indices of GaN, Ga-doped ZnO, and ITO are 2.4, 2.0, and 1.7, respectively [32]. The 500-nm-thick Ga-doped ZnO layer includes many nanofits in the film. Thus, the effective refractive index of the 500-nm-thick Ga-doped ZnO can be estimated by the effective medium theory as following Eq. (3) [15,33],

$$n_{eff\_LED\,C} = [n_{ZnO:Ga\,(LED\,B)}{}^2 V_{ZnO:Ga\,(LED\,B)} + n_{air}{}^2 (1 - V_{ZnO:Ga\,(LED\,B)})]^{1/2} \tag{3}$$

where $n_{ZnO:Ga\,(LED\,B)}$ and n_{air} are the refractive indices of Ga-doped ZnO and air, respectively, and $V_{ZnO:Ga}$ is the volume fraction of Ga-doped ZnO. Based on SEM images of LED C [Fig. 1(d) and 1(e)], the volume fraction of 500-nm-thick Ga-doped ZnO (LED C) was estimated to

Optics EXPRESS

be 0.73. From the effective medium theory, the effective refractive index of 500-nm-thick Ga-doped ZnO (LED C) is calculated to be 1.91, and this value is slightly lower than that of 180-nm-thick Ga-doped ZnO ($n_{ZnO:Ga\,(LED\,B)} = 20$) but it is still higher than that of ITO ($n_{ITO\,(LED\,A)} = 1.7$). Therefore, the increased optical transmittance of the Ga-doped ZnO films compared with that of ITO is attributed to the enhanced light extraction from *p*-GaN by the Ga-doped ZnO TCL, which has a higher critical angle than that of the ITO TCL. Meanwhile, the transmittance of the Ga-doped ZnO films slightly decreases with increasing film thickness from 180 to 500 nm because of the decreased effective refractive index, point defects (oxygen vacancies) and disorder in the Ga-doped ZnO layer and the increased light absorption caused by light scattering [34].

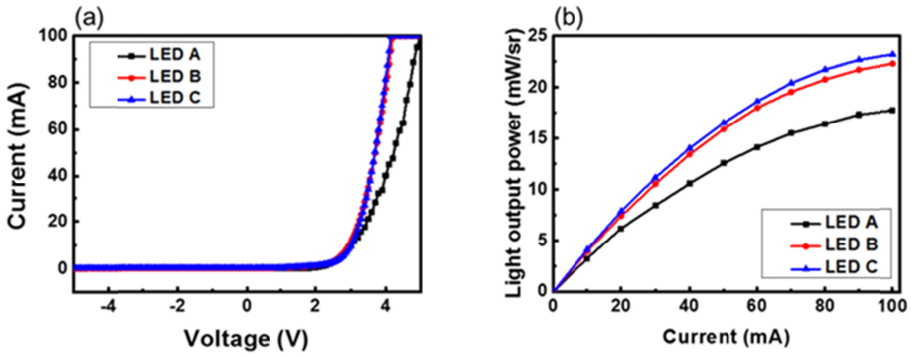

Fig. 6. (a) *I-V* characteristics and (b) optical output power of LED A, B, and C.

The current–voltage (*I-V*) characteristics and light output power, respectively, of the three LEDs as shown in Fig. 6(a) and 6(b). Figure 6(a) reveals that the forward voltages of LED A, B, and C at 20 mA were 3.42, 3.23, and 3.28 V, respectively. The lower forward voltages of LED B and C compared with that of LED A are attributed to the increased carrier concentration, mobility and the reduced resistivity. Hall effect measurements showed the resistivity, carrier concentration and mobility in each TCL are 3.1×10^{-4} Ω·cm, 1.64×10^{19} cm^{-3} and 6.07 $cm^2/V{\cdot}s$ for LED A, 5.3×10^{-4} Ω·cm, 2.31×10^{19} cm^{-3} and 32.8 $cm^2/V{\cdot}s$ for LED B, and 5.2×10^{-4} Ω·cm, 2.87×10^{20} cm^{-3} and 23.7 $cm^2/V{\cdot}s$ for LED C, respectively. It has been reported that the carrier mobility and concentration of Ga-doped ZnO after thermal annealing increases because of the decomposition of structural defects in the Ga-doped ZnO TCL [16]. Therefore, the decreased carrier mobility of LED C compared with that of LED B is attributed to the increased carrier concentration in the Ga-doped ZnO TCL, which led to electron–electron scattering [35,36]. Figure 6(b) indicates the light output power of LED B and C at 100 mA is increased by 26.9% and 30.9%, respectively, compared with that of LED A. The increase of light output power of LED B and C is attributed to the enhanced radiative recombination caused by the relaxation of compressive strain in the MQW active region and the increased light extraction from the Ga-doped ZnO TCL.

Optics EXPRESS

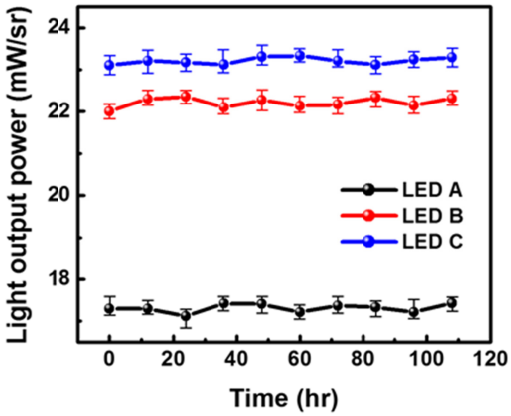

Fig. 7. Optical output power of three LEDs as a function of time under ambient conditions.

The stability of the optical output power of LEDs with three TCLs was studied over the period of 5 days in time intervals of 12 hours under ambient condition as shown in Fig. 7. During this experiment, the optical output power of LEDs with three TCLs remained constant, indicating the good long-term stability and repeatability of the optical properties in Ga-doped ZnO TCLs. Jen et al. also reported that the electrical stability (carrier concentration, mobility, and conductivity) of Ga-doped ZnO film was highly stable over a period of 250 days because the occupation of oxygen vacancies could be activated only at high temperature of 500 °C [37].

4. Conclusion

In conclusion, we demonstrated high-performance InGaN/GaN MQW LEDs with Ga-doped ZnO TCLs. Lower forward voltages of 3.23 and 3.28 V were observed at 20 mA for LED B and C compared to 3.42 V for LED A with an ITO TCL because of the increased carrier concentration and mobility in the Ga-doped ZnO TCLs. The output power of the LED with a 500-nm-thick Ga-doped ZnO TCL was increased by 30.9% at 100 mA compared to that of the reference LED with an ITO TCL. This improvement is attributed to the increased IQE achieved by the relaxation of compressive strain in the InGaN/GaN MQW region and increased LEE originating from the higher refractive index of the Ga-doped ZnO TCL than that of the ITO TCL. These results indicate that LEDs with Ga-doped ZnO TCLs are promising to aid realization of high-efficiency and high-power GaN-based LEDs.

Funding

Gwangju Institute of Science and Technology (GIST) (Amano Center for Advanced LED); Basic Science Research Program through the National Research Foundation of Korea (NRF) funded by the Ministry of Education (NRF-2017R1A2B2011858).

References

1. E. F. Schubert and J. K. Kim, "Solid-state light sources getting smart," Science **308**(5726), 1274–1278 (2005).
2. F. A. Ponce and D. P. Bour, "Nitride-based semiconductors for blue and green light-emitting devices," Nature **386**(6623), 351–359 (1997).
3. M. H. Kim, M. F. Schubert, Q. Dai, J. K. Kim, E. F. Schubert, J. Piprek, and Y. Park, "Origin of efficiency droop in GaN-based light-emitting diodes," Appl. Phys. Lett. **91**(18), 183507 (2007).
4. X. Da, X. Guo, L. Dong, Y. Song, W. Ai, and G. Shen, "The silicon oxynitride layer deposited at low temperature for high-brightness GaN-based light-emitting diodes," Solid-State Electron. **50**(3), 508–510 (2006).
5. C. Y. Cho, S. J. Lee, S. H. Hong, S. C. Park, S. E. Park, Y. Park, and S. J. Park, "Growth and separation of high quality GaN epilayer from sapphire substrate by lateral epitaxial overgrowth and wet chemical etching," Appl. Phys. Express **4**(1), 012104 (2011).

Optics EXPRESS

6. M. K. Kwon, J. Y. Kim, B. H. Kim, I. K. Park, C. Y. Cho, C. C. Byeon, and S. J. Park, "Surface-plasmon-enhanced light-emitting diodes," Adv. Mater. **20**(7), 1253–1257 (2008).
7. S. J. Lee, C. Y. Cho, S. H. Hong, S. H. Han, S. Yoon, S. T. Kim, and S. J. Park, "Enhanced optical power of InGaN/GaN light-emitting diode by AlGaN interlayer and electron blocking layer," IEEE Photonics Technol. Lett. **24**(22), 1991–1994 (2012).
8. J. Y. Kim, M. K. Kwon, K. S. Lee, S. J. Park, S. H. Kim, and K. D. Lee, "Enhanced light extraction from GaN-based green light-emitting diode with photonic crystal," Appl. Phys. Lett. **91**(18), 181109 (2007).
9. T. X. Lee, K. F. Gao, W. T. Chien, and C. C. Sun, "Light extraction analysis of GaN-based light-emitting diodes with surface texture and/or patterned substrate," Opt. Express **15**(11), 6670–6676 (2007).
10. Z. Szabó Z. Baji, P. Basa, Z. Czigany, I. Barsony, H.-Y. Wang, and J. Volk, "Homogeneous transparent conductive ZnO:Ga by ALD for large LED wafers," Appl. Surf. Sci. **379**, 304–308 (2016).
11. J. W. Kang, M. S. Oh, Y. S. Choi, C. Y. Cho, T. Y. Park, C. W. Tu, and S. J. Park, "Improved light extraction of GaN-based green light-emitting diodes with an antireflection layer of ZnO nanorod arrays," Electrochem. Solid-State Lett. **14**(3), H120–H123 (2011).
12. W. Gu, X. Wu, and J. Zhang, "Low resistance Ga-doped ZnO ohmic contact to *p*-GaN by reducing the sputtering power," Mater. Sci. Semicond. Process. **81**, 89–93 (2018).
13. Y. Kashiwaba, F. Katahira, K. Haga, T. Sekiguchi, and H. Watanabe, "Hetero-epitaxial growth of ZnO thin flms by atmospheric pressure CVD method," J. Cryst. Growth **221**(1-4), 431–434 (2000).
14. R. H. Horng, K.-C. Shen, C.-Y. Yin, C.-Y. Huang, and D.-S. Wuu, "High performance of Ga-doped ZnO transparent conductive layers using MOCVD for GaN LED applications," Opt. Express **21**(12), 14452–14457 (2013).
15. Y. C. Leem, N.-Y. Kim, W. Lim, S.-T. Kim, and S. J. Park, "Enhanced optical output power of InGaN/GaN vertical light-emitting diodes by ZnO nanorods on plasma-treated N-face GaN," Nanoscale **6**(17), 10187–10192 (2014).
16. C.-Y. Cho, N.-Y. Kim, J.-W. Kang, Y.-C. Leem, S.-H. Hong, W. Lim, S.-T. Kim, and S. J. Park, "Improved light-extraction efficiency in blue light-emitting diodes by SiO_2-coated ZnO nanorod arrays," Appl. Phys. Express **6**(4), 042102 (2013).
17. T. Y. Park, Y. S. Choi, S. M. Kim, G. Y. Jung, S. J. Park, B. J. Kwon, and Y. H. Cho, "Electroluminescence emission from light-emitting diode of *p*-ZnO/(InGaN/GaN) multiquantum well/*n*-GaN," Appl. Phys. Lett. **98**(25), 251111 (2011).
18. T. Y. Park, Y. S. Choi, J. W. Kang, J. H. Jeong, S. J. Park, D. M. Jeon, J. W. Kim, and Y. C. Kim, "Enhanced optical power and low forward voltage of GaN-based light-emitting diodes with Ga-doped ZnO transparent conducting layer," Appl. Phys. Lett. **96**(5), 051124 (2010).
19. H. Deng, J. J. Russell, R. N. Lamb, B. Jiang, Y. Li, and X. Y. Zhou, "Microstructure control of ZnO thin films prepared by single source chemical vapor deposition," Thin Solid Films **458**(1-2), 43–46 (2004).
20. A. G. Kontos, Y. S. Raptis, N. T. Pelekanos, A. Georgakilas, E. Bellet-Amalric, and D. Jalabert, "Micro-Raman characterization of $In_xGa_{1-x}N/GaN/Al_2O_3$ heterostructures," Phys. Rev. B Condens. Matter Mater. Phys. **72**(15), 155336 (2005).
21. L. Y. Chen, H. H. Huang, C. H. Chang, Y. Y. Huang, Y. R. Wu, and J. Huang, "Investigation of the strain induced optical transition energy shift of the GaN nanorod light emitting diode arrays," Opt. Express **19**(4), 900–907 (2011).
22. S. Watanabe, N. Yamada, M. Nagashima, Y. Ueki, C. Sasaki, Y. Yamada, T. Taguchi, K. Tadatomo, H. Okagawa, and H. Kudo, "Internal quantum efficiency of highly-efficient $In_xGa_{1-x}N$-based near-ultraviolet light-emitting diodes," Appl. Phys. Lett. **83**(24), 4906–4908 (2003).
23. P. M. McBride, Q. Yan, and C. G. Van de Walle, "Effects of In profile on simulations of InGaN/GaN multi-quantum-well light-emitting diodes," Appl. Phys. Lett. **105**(8), 083507 (2014).
24. Y.-H. Sun, Y.-W. Cheng, S.-C. Wang, Y.-Y. Huang, C.-H. Chang, S.-C. Yang, L.-Y. Chen, M.-Y. Ke, C.-K. Li, Y.-R. Wu, and J. J. Huang, "Optical properties of the partially strain relaxed InGaN/GaN light-emitting diodes induced by *p*-type GaN surface texturing," IEEE Electron Device Lett. **32**(2), 182–184 (2011).
25. Q. Wang, J. Bai, Y. P. Gong, and T. Wang, "Influence of strain relaxation on the optical properties of InGaN/GaN multiple quantum well nanorods," J. Phys. D Appl. Phys. **44**(39), 395102 (2011).
26. J. H. Son, J. L. Lee, and J. N. Lee, "Strain engineering for the solution of efficiency droop in InGaN/GaN light-emitting diodes," Opt. Express **18**(6), 5466–5471 (2010).
27. T. Mukai, M. Yamada, and S. Nakamura, "Current and temperature dependences of electroluminescence of InGaN-Based UV/blue/green light-emitting diodes," Jpn. J. Appl. Phys. **37**(Part 2, No. 11B), L1358–L1361 (1998).
28. S. J. Kim, K. J. Lee, and S. J. Park, "Alleviation of efficiency droop in InGaN/GaN multiple quantum well light-emitting diodes with trapezoidal quantum barriers," J. Phys. D Appl. Phys. **51**(25), 25LT01 (2018).
29. Z. Lin, H. Wang, S. Chen, Y. Lin, M. Yang, G. Li, and B. Xu, "Achieving high-performance blue GaN-based light-emitting diodes by energy band modification on $Al_xIn_yGa_{1-x-y}N$ electron blocking layer," *IEEE* Trans. Electron Devices **64**(2), 472–480 (2017).
30. R. A. Red'ko, "Optical approach to analysis of interaction of gallium nitride and weak magnetic fields," Funct. Mater. **22**(2), 188–192 (2015).

Optics EXPRESS

31. R. Redko, G. Milenin, V. Milenin, R. Konakova, S. Redko, P. Lytvyn, and O. Babenko, "Modification of GaN thin film on sapphire substrate optical properties under weak magnetic fields," Mater. Res. Express **6**, 036412 (2019).
32. Z. Yin, X. Liu, H. Wang, Y. Wu, X. Hao, Z. Ji, and X. Xu, "Light transmission enhancement from hybrid ZnO micro-mesh and nanorod arrays with application to GaN-based light-emitting diodes," Opt. Express **21**(23), 28531–28542 (2013).
33. D.-S. Tsai, C.-A. Lin, W.-C. Lien, H.-C. Chang, Y.-L. Wang, and J.-H. He, "Ultra-high-responsivity broadband detection of Si metal-semiconductor-metal Schottky photodetectors improved by ZnO nanorod arrays," ACS Nano **5**(10), 7748–7753 (2011).
34. Y.-J. Lin, C.-L. Tsai, Y.-M. Lu, and C.-J. Liu, "Optical and electrical properties of undoped ZnO films," J. Appl. Phys. **99**(9), 093501 (2006).
35. K.-W. Seo, H.-S. Shin, J.-H. Lee, K.-B. Chung, and H.-K. Kim, "The effects of thickness on the electrical, optical, structural and morphological properties of Al and Ga co-doped ZnO films grown by linear facing target sputtering," Vacuum **101**, 250–256 (2014).
36. C. Hilsum, "Simple empirical relationship between mobility and carrier concentration," Electron. Lett. **10**(13), 259–260 (1974).
37. S.-U. Jen, H. Sun, H.-P. Chiang, S.-C. Chen, J.-Y. Chen, and X. Wang, "Optoelectronic properties and the electrical stability of Ga-doped ZnO Thin Films prepared via radio frequency sputtering," Materials (Basel) **9**(12), 987–995 (2016).